J. Phys. Chem. A **2001,** *105,* 2142−2146

ARTICLES

Do Nitrogen-Atom-Containing Endohedral Fullerenes Undergo the Shrink-Wrap Mechanism?[†]

Baopeng Cao,[‡] Tikva Peres,[‡] R. James Cross, Jr.,[§] Martin Saunders,[§] and Chava Lifshitz*,[‡]

Department of Physical Chemistry and The Farkas Center for Light Induced Processes,
The Hebrew University of Jerusalem, Jerusalem 91904, Israel, and Department of Chemistry,
Yale University, New Haven, Connecticut 06520-8107

Received: April 7, 2000; In Final Form: June 20, 2000

The endohedral nitrogen-atom-containing fullerenes, N@C_{60} and N@C_{70}, were studied mass spectrometrically. The neutral endohedrals are thermally unstable. This instability can be followed by mass spectrometry as well as by EPR spectroscopy. The corresponding ions were studied by using mass-analyzed ion kinetic energy (MIKE) spectroscopy. Unlike metal-containing and noble-gas-containing endohedral fullerenes studied earlier, the ions N@$C_{60}{}^+$ and N@$C_{70}{}^+$ do not lose C_2 groups unimolecularly but lose the nitrogen atom instead. This indicates that the activation energy for nitrogen-atom loss is lower than that for the C_2 elimination from the cage. This was verified through the analysis of kinetic energy release distribution (KERD) measurements. The results are discussed in light of the thermal instability of nitrogen-atom-containing endohedral compounds compared to noble-gas-containing analogues.

Introduction

One of the fascinating properties of fullerenes is their ability to trap atoms and small molecules inside the cage. The first evidence for endohedral metallofullerenes was reported soon after the discovery of C_{60}.[1] These compounds are stabilized by the transfer of electrons from the metal to the carbon cage.[2,3] They are prepared by adding the appropriate materials during the formation of the fullerenes. An alternative method involves the application of high temperatures and high pressures for the encapsulation of noble gas atoms into C_{60}.[4] In the latter compounds, the endohedral atoms are trapped inside the fullerene because the holes in the cage are too small for them to escape. Endohedral compounds can also be prepared by ion implantation. This technique has been applied to lithium and other alkali atom fullerenes,[5] to noble gas fullerenes,[6a] and to noble-gas-containing dodecahedrane.[6b]

A particularly interesting endohedral compound that has been produced by the ion implantation technique is N@C_{60}.[7] The most distinct feature of N@C_{60} is that an extremely reactive atom (atomic nitrogen) is stabilized in its electronic ground-state configuration by the protective shielding of C_{60}.[8] The fullerenes are protective cages for the atomic nitrogen that have been termed “chemical Faraday cages”.[9] Because the encapsulated atom keeps its atomic structure, the EPR (electron paramagnetic resonance) technique was found to be extremely useful in the investigation of this system.[9−11]

Mass spectrometry has played a central role in the study of endohedral fullerenes.[3−5,12] The discovery of C_{60} was based on a prominent peak in the mass spectrum at a mass-to-charge ratio, *m/z*, of 720.[13,14] Yet, to the best of our knowledge, there has been no serious mass spectrometric study of N@C_{60} or N@C_{70}. The earliest experiments yielded a concentration of only 10^{-7} paramagnetic centers per C_{60} molecule, and mass spectrometric identification of the complex was difficult.[7] The N@C_{60} and N@C_{70} compounds are the topic of the present study. In addition to reporting on their electron impact induced mass spectra, we will concentrate on their gas-phase ion chemistry—specifically, the unimolecular fragmentations obtained through MIKE (mass-analyzed ion kinetic energy) spectrometry. Fullerenes, endohedral fullerenes, and their respective cations are generally known to undergo consecutive C_2 eliminations in what used to be called the Rice shrink-wrap mechanism.[15,16] We would like to determine whether fullerenes containing an endohedral nitrogen atom undergo C_2 elimination.

Using the technique of MIKE spectrometry, it is possible to deduce kinetic energy release distributions (KERDs) for unimolecular decompositions. Modeling of these KERDs allows extraction of valuable information about the energetics and dynamics of the reactions involved. The C_2 binding energies of the empty fullerenes, endohedral metallofullerenes, and noble gas endohedral fullerenes have been deduced from such experiments.[17−19] Similar experiments performed on N@C_{60} and N@C_{70} are reported here.

Experimental Section

1. Preparation of N@C_{60} and N@C_{70}. The apparatus for preparing endohedral compounds by the ion implantation technique has been described in detail previously.[6] The reaction takes place on a rotating aluminum cylinder. On one side is an oven producing a continuous beam of fullerene, which con-

---

[†] Part of the special issue “Aron Kuppermann Festschrift”.

* Author to whom correspondence should be addressed.

[‡] The Hebrew University of Jerusalem.

[§] Yale University.

10.1021/jp001359c CCC: $20.00 © 2001 American Chemical Society
Published on Web 08/23/2000

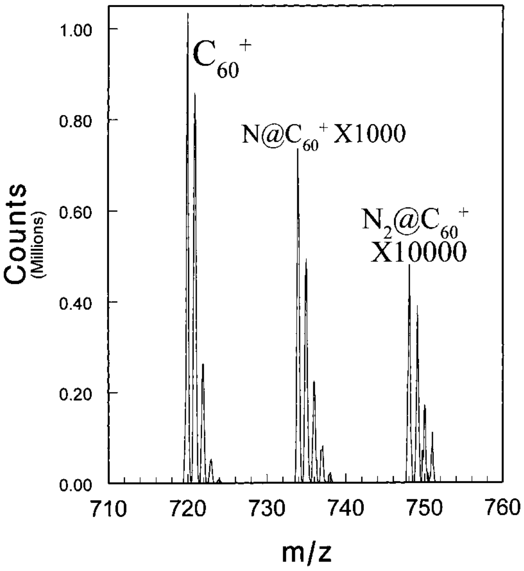

Figure 1. Mass spectrum of a $N@C_{60}$-containing fullerene sample made by N^+ ion-beam implantation into C_{60}.

denses on the cylinder. A source of atomic nitrogen ions is mounted on the other side of the target. The beam of N^+ is made by passing N_2 through an electrical discharge. The ions are then accelerated to 200 eV, and they slam into the fullerene surface. After a few hours, the apparatus is opened, and the target is removed. The endohedral character of the N atom inside the fullerene cage is verified by EPR experiments. Combining the results of several separate beam runs increases the amount of enriched endohedral sample.

2. Mass Spectrometry and MIKE Spectrometry. Measurements were performed on a high-resolution double-focusing mass spectrometer of reversed geometry, the VG-ZAB-2F,[20,21] running mass spectra at a very high dynamic range as well as using the technique of MIKE spectrometry. The endohedral fullerene cations were obtained by ionization of the corresponding neutral samples.

The samples were introduced into the mass spectrometer using the direct insertion probe and evaporated at 400 °C. The electron-impact conditions were as follows: electron ionizing energy, 70 eV; emission current, 5 mA; ion source temperature, 400 °C; and resolution, 1100 (10% valley definition). Metastable ion peakshapes were determined by scanning the electrostatic analyzer and using single-ion counting. Ion counting was achieved by a combination of an electron multiplier, amplifier/discriminator, and multichannel analyzer.[22] The experiments were performed at 8-kV acceleration voltage and a main beam width of 1.5−5 V. The data were accumulated in a computer-controlled experiment, monitoring the main beam scan and correcting for the drift of the main beam.[21] The metastable ion peak shapes were mean values of 10−100 accumulated scans. The product KERDs were determined from the first derivatives of the metastable ion peak shapes.[23−25]

Results and Discussion

1. Mass Spectra and Thermal Stability. The combination of the ZAB-2F mass spectrometer with ion counting and with the multichannel analyzer allowed the detection of even very low degrees of incorporation into the fullerene cage, because of the very wide dynamic range achieved. Figure 1 demonstrates this for $N@C_{60}$ that has been prepared by the ion-beam implantation technique. Beginning at *m*/*z* 734, Figure 1 shows for the first time the presence of a series of small peaks, whose relative intensities can be fit knowing the isotopic abundance of ^{13}C that is the unique signature of $N@C_{60}^+$. The ratio of filled to empty fullerene is seen to be about 1:1400 for $N@C_{60}$. This concentration is between about 1 and 2 orders of magnitude higher than some of the earlier results reported on the basis of EPR measurements.[8] Because the N^+ beam is made from molecular nitrogen, there is a small but discernible signal of $N_2@C_{60}^+$, the ratio of filled to empty fullerene being 1:21 000 for $N_2@C_{60}$ for this specific sample. It is worthwhile mentioning that we have previously seen $N_2@C_{60}^+$ signals from $N_2@C_{60}$ prepared from molecular nitrogen and C_{60} by the high-pressure process.

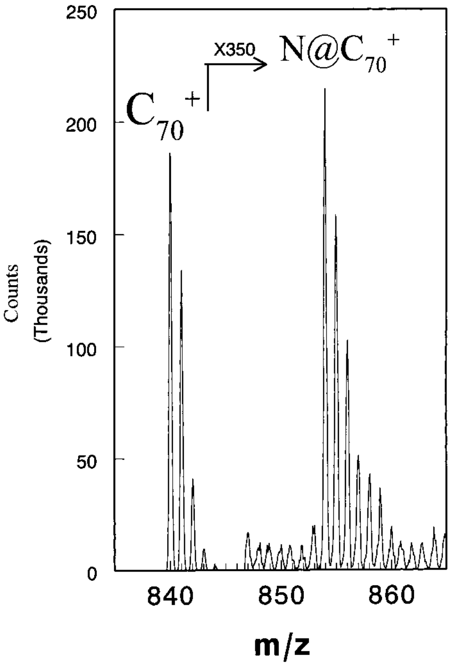

Figure 2. Mass spectrum of a $N@C_{70}$-containing fullerene sample made by N^+ ion-beam implantation into C_{70}.

The degree of incorporation of nitrogen atoms into C_{70} is somewhat higher than that for C_{60} under similar experimental conditions. The ratio of the filled $N@C_{70}$ to the empty C_{70} fullerene is about 1:300 (Figure 2).

$N@C_{60}$ is stable at room temperature at ambient conditions, and no loss of the EPR signal intensity is observed after storage for several months in the dark. Above 500 K, however, the EPR signal intensity starts to decrease on a time scale of minutes.[26] We were interested to determine whether the mass spectrometric signal is also lost following a heating period. An experiment was done by accurately dividing a sample in half; one-half was heated at 230 C for 4 h, while the other half was used as a control. The EPR data for the heated and unheated parts were carefully analyzed. The ratio of EPR intensities of the heated to unheated samples was found to be 0.103 ± 0.004, indicating the loss upon heating of the free nitrogen atom inside the cage. The same two samples were subjected to mass spectrometric studies. The mass spectrometric ratio of nitrogen-atom-containing fullerene to empty fullerene decreased by a factor of 0.17 upon heating. There are two important conclusions from this observation: (1) Although we are heating the samples in the ion source, the degree of loss of the nitrogen atom over the short period of mass spectrometric analysis is not critical. (We do observe, however, a loss of the ion signal upon prolonged heating of the sample in the ion source.) (2) Loss of the EPR signal is due to loss of the nitrogen atom from the cage. No alternative nitrogen-containing C_{60} isomer is formed. If it were

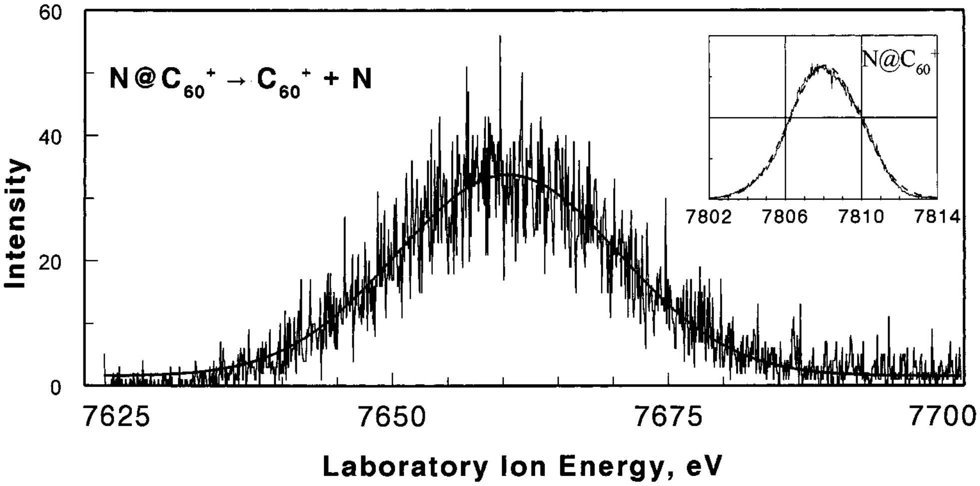

Figure 3. Metastable ion peak shape for the indicated reaction of loss of the endohedral nitrogen atom from $N@C_{60}^+$ taking place in the second field-free region of the VG-ZAB-2F obtained through a MIKE scan of the electrostatic analyzer. The precursor parent ion peak shape is given in the inset.

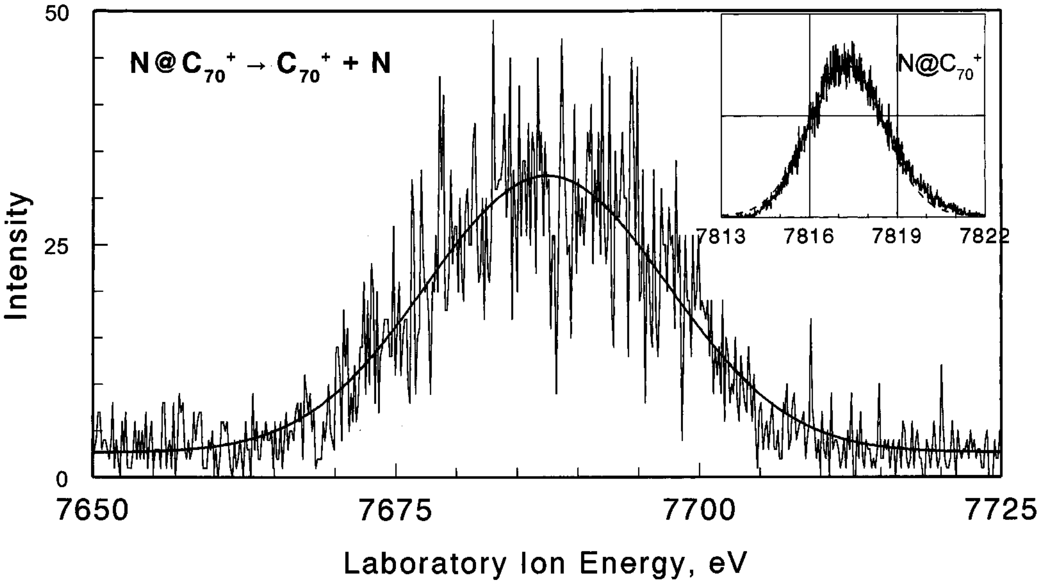

Figure 4. Metastable ion peak shape for the indicated reaction of $N@C_{70}^+$ taking place in the second field-free region of the VG-ZAB-2F obtained through a MIKE scan of the electrostatic analyzer. The precursor parent ion peak shape is given in the inset.

formed, then the loss of the EPR signal would not be accompanied by a similar loss in the mass spectrometric signal at the mass-to-charge position corresponding to the endohedral species. We do not claim that we are observing the neutral analogue to reaction 1a, as we cannot observe the products. The nitrogen atom will almost certainly react on the outside of the fullerene double bond to form a CCN three-membered ring that is an exposed free radical. The latter can then react with another fullerene to form a nonvolatile polymer that would not show up in the mass spectrum. Even if it were a free radical, the EPR spectrum would be smeared out and probably unobservable.

The present data are the first efforts we are aware of in the direction of mass spectrometry of the nitrogen-atom-containing endohedral fullerenes. It is particularly interesting to study the unimolecular reactions of $N@C_{60}^+$ and $N@C_{70}^+$ described in the next section to see how different they are from those of the endohedral metallofullerenes and the noble-gas-containing endohedral fullerenes, which have been demonstrated to lose C_2.[18]

2. Unimolecular Decompositions of $N@C_{60}^+$ and $N@C_{70}^+$. In principle, there should be competition among the unimolecular reactions of endohedral fullerenes between the elimination of the endohedral atom and the loss of a C_2 unit from the cage. For example, in the case of $N@C_{60}^+$, there are two possible channels

$$N@C_{60}^+ \rightarrow C_{60}^+ + N \tag{1a}$$

$$N@C_{60}^+ \rightarrow N@C_{58}^+ + C_2 \tag{1b}$$

MIKE spectrometry is a powerful technique for determining which channel the endohedral fullerenes follow in their unimolecular reactions. Figure 3 represents the metastable ion peak shape for the dissociation taking place in the second field-free region of the ZAB-2F. The position of the maximum of the metastable ion peak is at 7660.5 eV, whereas the parent ion peak is at 7808.1 eV laboratory energy. From the known mass of the reactant parent ion (m/z 734) and the ratio of kinetic energies (0.981), the product ion mass is calculated to be 720. In other words, the reaction is 1a, the clean elimination of a nitrogen atom leading to C_{60}^+. No other fragmention channel was observed for $N@C_{60}^+$. The endohedral ion $N@C_{70}^+$ undergoes a similar elimination of the nitrogen atom, reaction

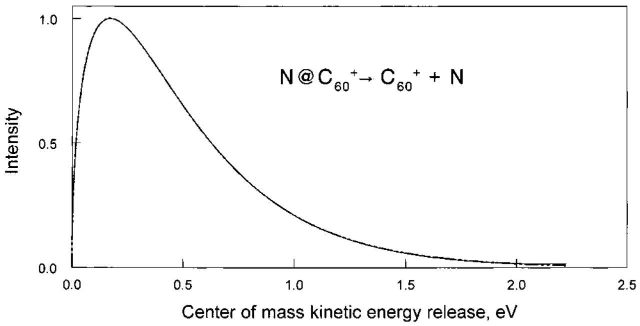

Figure 5. Center-of-mass kinetic energy release distribution for loss of the endohedral nitrogen atom from $N@C_{60}^+$.

2a, (Figure 4)

$$N@C_{70}^+ \rightarrow C_{70}^+ + N \tag{2a}$$

The loss of the endohedral atom is quite different from the usual behavior of endohedral metallofullerenes and noble-gas-containing endohedral fullerenes, which undergo C_2 elimination and do not lose the endohedral atom before they reach a critical size.

3. Kinetic Energy Releases. Unimolecular reactions that possess no reverse activation energies lead to kinetic energy release distributions (KERDs) that are Boltzmann-like and can be modeled by statistical theories. In the model-free approach, the KERD is written in the form[18]

$$p(\epsilon) = \epsilon^l \exp(-\epsilon/k_B T^{\ddagger}) \quad (0 < l < 1) \tag{3}$$

where ϵ is the kinetic energy release, l is a parameter that ranges from zero to unity, k_B is the Boltzmann constant, and $T^{\ddagger}$ is the transition state temperature defined by the average kinetic energy on passage through the transition state. The values of l and $T^{\ddagger}$ are obtained by fitting the experimental KERD with eq 3. The value of l that was found to give the best fit for all of the KERDs is $l \cong 0.5$. This corresponds to the expected value for the most statistical situation, as the translational density of states is proportional[27] to $\epsilon^{0.5}$.

The isokinetic bath temperature is defined in finite heat bath theory (FHBT) as the temperature to which a heat bath should be set so that the canonical rate constant, $k(T_b)$, is equal to the microcanonical rate constant, $k(E)$, sampled in the experiment. The isokinetic bath temperature is given by[28,29]

$$T_b = T^{\ddagger} \frac{\exp(\gamma/C) - 1}{\gamma/C} \tag{4}$$

where C is a dimensionless heat capacity and γ is the Gspann parameter.[30] The vaporization energy, ΔE_{vap} (that can be equated with the activation energy), and the isokinetic bath temperature are connected via the Trouton relation

$$\Delta E_{vap} = \gamma k_B T_b \tag{5}$$

A typical KERD obtained for reaction 1a is presented in Figure 5. The modeled KERD (eq 3) is superimposed on the experimental curve (Figure 5). Several experiments of this type under the highest possible energy resolutions were combined, and the following results were derived: average kinetic energy release, $\langle\epsilon\rangle_{(1a)} = 0.51 \pm 0.02$ eV; transition state temperature, $T^{\ddagger}(1a) = 4000 \pm 240$ K; and parameter $l = 0.50 \pm 0.01$. The C_2 evaporation from C_{60}^+, reaction 6

$$C_{60}^+ \rightarrow C_{58}^+ + C_2 \tag{6}$$

was run under similar conditions of energy resolution, and the corresponding values obtained were: $\langle\epsilon\rangle_{(6)} = 0.45 \pm 0.02$ eV; $T^{\ddagger}(6) = 3500 \pm 200$; and $l = 0.50 \pm 0.00$.

4. Binding Energies and Activation Energies. In a recent review paper[31] of the current status of the C_2 binding energy in C_{60}^+, we have come to the conclusion that $\Delta E_{vap}(C_{60}^+) \geq 9.5$ eV. Because C_2 evaporation from $N@C_{60}^+$, reaction 1b, does not compete with reaction 1a, it must be concluded that the evaporation energy of the nitrogen atom from $N@C_{60}^+$ (i.e., the activation energy for reaction 1a) is lower than that for C_2 evaporation. It must be pointed out, however, that the values of the evaporation energy of C_2 from C_{60}^+ and from $N@C_{60}^+$ might not necessarily be equal.[18] If they are nearly equal, then a value of about 9.5 eV should be considered as an upper limit for the activation energy of reaction 1a.

The Gspann parameter defines the degree of looseness of the transition state, as

$$\ln A - \ln k(T_b) = \gamma \tag{7}$$

where A is the Arrhenius preexponential factor. Reaction 6 has been demonstrated[31] to possess a very loose transition state with a high Gspann parameter, $\gamma(6) = 33$. Using eqs 4 and 5 with the preferred Gspann parameter for reaction 6,[31] $\gamma(6) = 33$, and the present experimental kinetic energy release data for reaction 6 gives $\Delta E_{vap}(C_{60}^+) = 11.0 \pm 0.6$ eV. This value is somewhat higher than, but within error limits of, previous determinations[19,31] of the binding energy of C_2 in C_{60}^+.

The degree of looseness of the transition state for reaction 1a is unknown. It is conceivable that γ for reaction 1a is considerably lower than 33. One reason is that there are 60 ways of choosing the reaction coordinate in the case of reaction 6, i.e., the reaction path degeneracy[31] is $\sigma = 60$, whereas σ is presumably 1 for reaction 1a. Taking $\gamma(1a) = 33 - \ln 60 = 28.9$ and using eqs 4 and 5 with the kinetic energy release data for reaction 1a, one obtains $\Delta E_{vap}(1a) = 10.8 \pm 0.6$ eV. This is again an upper limit for two reasons: (1) In view of the very low intensities of the nitrogen endohedral samples, some energy resolution was sacrificed in favor of increased sensitivity. This leads to increased metastable ion peak widths and increasing vaporization energies deduced therefrom. (2) The transition state for reaction 1a is probably not as loose as the one for reaction 6 or 1b (see ref 31 for a detailed discussion of the looseness of the transition state for C_2 elimination, reaction 6). A γ value of 28.9 corresponds to a preexponential A factor of $A = 3.5 \times 10^{17}$ s^{-1}, as the most probable rate constant is $k(T_b) \approx 10^5$ s^{-1}. Such a high A factor is very unlikely for reaction 1a. If the preexponential A factor for reaction 1a is as low as has been assumed for its neutral analogue,[32] $A = 10^{13}$ s^{-1}, then $\gamma(1a) = 18.4$. Using eqs 4 and 5, one then obtains a lower limit on the binding (activation) energy of reaction 1a, $\Delta E_{vap}(1a) = 6.7$ eV. These arguments place the activation energy for reaction 1a in the range $6.7 \leq \Delta E_{vap}(1a) \leq 11.0$ eV. Restricting the range of values of the preexponential A factor and of the Gspann parameter γ further would restrict the range of activation energies deduced.

The behavior of the nitrogen-atom-containing endohedral ions that lose the nitrogen atom unimolecularly rather than by evaporating C_2 is quite unique but is entirely in agreement with the thermal instability of the corresponding neutrals.[26,32] Whereas relatively mild heating of $N@C_{60}$ leads to the release of the nitrogen atom from the cage, the extrusion of He from $He@C_{60}$ requires thermal treatment for hours at 900−1150 K and is accompanied by an irreversible destruction of the fullerene cage. It has been demonstrated computationally[32] that the nitrogen atom escapes the cage via formation of intermediates that are covalently bound adducts with endohedral aza bridges. An autocatalytic bond breakage ensues that requires less energy than the considerable cage distortion needed for penetration by helium. A similar autocatalytic mechanism may prevail in the case of the ionic species. The result is that the activation energy for loss of the endohedral atom from $N@C_{60}^+$ is lower than the evaporation energy of C_2, whereas the reverse is true for $He@C_{60}^+$. The activation energy calculated from the KERD measurements, $6.7 \leq \Delta E_{vap}(1a) \leq 11.0$ eV, is indeed lower than the C_2 evaporation energy, but is considerably higher than the Arrhenius activation energy deduced or energy barriers calculated,[32] 40−67 kcal/mol for the escape of N from neutral $N@C_{60}$. Additional studies are clearly required to establish the energetics on a firmer basis.

Acknowledgment. This research was supported by The Hebrew University Intramural Research Fund Basic Project Awards. Dr. Baopeng Cao thanks The Hebrew University for the award of a Golda Meir Postdoctoral fellowship. The work at Yale was supported by the National Science Foundation and by the Petroleum Research Fund. The Farkas Research Center is supported by the Minerva Gesellschaft für die Forschung GmbH, München, Germany.

References and Notes

(1) Heath, J. R.; O'Brien, S. C.; Zhang, Q.; Liu, Y.; Curl, R. F.; Kroto, H. W.; Tittel, F. K.; Smalley, R. E. *J. Am. Chem. Soc*. **1985**, *107*, 7779.

(2) Johnson, R. D.; de Vries, M. S.; Salem, J. R.; Bethune, D. S.; Yanoni, C. S. *Nature* **1992**, *355*, 239.

(3) Bethune, D. S.; Johnson, D. S.; Salem, J. R.; de Vries, M. S.; Yannoni, C. S. *Nature* **1993**, *366*, 123.

(4) Saunders, M.; Jiménez-Vázquez, H. A.; Cross, R. J.; Poreda, R. J. *Science* **1993**, *259*, 1428.

(5) Teligmann, R.; Krawez, N.; Lin, S.-H.; Hertel, I. V.; Campbell, E. E. B. *Nature* **1996**, *382*, 407.

(6) (a) Shimshi, R.; Cross, R. J.; Saunders: M. *J. Am. Chem. Soc.* **1997**, *119*, 1163. (b) Cross, R. J.; Saunders: M.; Prinzbach, H. *Org. Lett.* **1999**, *1*, 1479.

(7) Almeida Murphy, T.; Pawlik, Th.; Weidinger, A.; Höhne, M.; Alcala, R.; Spaeth, J.-M. *Phys. Rev. Lett.* **1996**, *77*, 1075.

(8) Weidinger, A.; Waiblinger, M.; Pietzak, B.; Almeida Murphy, T. *Appl. Phys. A* **1998**, *66*, 1.

(9) Pietzak, B.; Waiblinger, M.; Almeida Murphy, T.; Weidinger, A.; Höhne, M.; Dietel, E.; Hirsch, A. *Chem. Phys. Lett.* **1997**, *279*, 259.

(10) Knapp, C.; Dinse, K.-P.; Pietzak, B.; Waiblinger, M.; Weidinger, A. *Chem. Phys. Lett.* **1997**, *272*, 433.

(11) Dietel, E.; Hirsch, A.; Pietzak, B.; Waiblinger, M.; Lips, K.; Weidinger, A.; Gruss, A.; Dinse, K.-P. *J. Am. Chem. Soc.* **1999**, *121*, 2432.

(12) Laskin, J.; Peres, T.; Lifshitz, C.; Saunders, M.; Cross, R. J.; Khong, A. *Chem. Phys. Lett.* **1998**, *285*, 7.

(13) Kroto, H. W.; Heath, J. R.; O'Brien, S. C.; Curl, R. F.; Smalley, R. E. *Nature* **1985**, *318*, 162.

(14) Kroto, H. *Science* **1988**, *242*, 1139.

(15) O'Brien, S. C.; Heath, J. R.; Curl, R. F.; Smalley, R. E. *J. Chem. Soc.* **1988**, *88*, 220.

(16) Smalley, R. E. *Acc. Chem. Res.* **1992**, *25*, 98.

(17) Laskin, J.; Jiménez-Vázquez, H. A.; Shimshi, R.; Saunders, M.; de Vries, M. S.; Lifshitz, C. *Chem. Phys. Lett.* **1995**, *242*, 249.

(18) Laskin, J.; Peres, T.; Khong, A.; Jiménez-Vázquez, H. A.; Cross, R. J.; Saunders, M.; Bethune, D. S.; de Vries, M. S.; Lifshitz, C. *Int. J. Mass Spectrom.* **1999**, *185/186/187*, 61.

(19) Matt, S.; Echt, O.; Sonderegger, M.; David, R.; Scheier, P.; Laskin, J.; Lifshitz, C.; Märk, T. D. *Chem. Phys. Lett*. **1999**, *303*, 379.

(20) Morgan, P. P.; Beynon, J. H.; Bateman, R. H.; Green, B. N. *Int. J. Mass Spectrom. Ion Phys.* **1978**, *28*, 171.

(21) Kirshner, N. J.; Bowers, M. T. *J. Phys. Chem.* **1987**, *91*, 2573.

(22) Lifshitz, C.; Louage, F. *J. Phys. Chem.* **1989**, *93*, 6533.

(23) Holmes, J. L.; Osborne, A. D. *Int. J. Mass Spectrom. Ion Phys.* **1977**, *23*, 189.

(24) Lifshitz, C.; Tzidony, E. *Int. J. Mass Spectrom. Ion Phys.* **1981**, *39*, 181.

(25) Jarrold, M. F.; Wagner-Redeker, W.; Allies, A. J.; Kirchner N. J.; Bowers, M. T. *Int. J. Mass Spectrom. Ion Processes* **1984**, *58*, 63.

(26) Lips, K.; Waiblinger, M.; Pietzak, B.; Weidinger, A. *Phys. Status Solidi A* **2000**, *177*, 81.

(27) (a) Levine, R. D.; Bernstein, R. B. *Molecular Reaction Dynamics and Chemical Reactivity*; Oxford University Press: New York, 1987; p 274−275. (b) Baer, T.; Hase, W. L. *Unimolecular Reaction Dynamics*; Oxford University Press, New York, 1996; p 173−174. (c) Urbain, P.; Remacle, F.; Leyh, B.; Lorquet, J. C. *J. Phys. Chem*. **1996,** *100*, 8003.

(28) Lifshitz, C. In *Current Topics in Ion Chemistry and Physics: Clusters*; Baer, T., Ng, C. Y., Powis, I., Eds.; John Wiley & Sons: New York, 1993.

(29) Klots, C. E. *Z. Phys. D* **1991**, *21*, 335.

(30) Klots, C. E. *Int. J. Mass Spectrom. Ion Processes* **1990**, *100*, 457.

(31) Lifshitz, C. C_2 Binding Energy in C_{60}. *Int. J. Mass Spectrom.* **2000**, *198*, 1.

(32) Mauser, H.; van Eikema Hommes, N. J. R.; Clark, T.; Hirsch, A.; Pietzak, B.; Weidinger, A.; Dunsch, L. *Angew. Chem., Int. Ed. Engl.* **1997**, *36*, 2835.